Different Anomeric Sugar Bound States of Maltose Binding Protein Resolved by a Cytolysin A Nanopore Tweezer

Xin Li[1], Kuo Hao Lee[1], Spencer Shorkey[1,2], Jianhan Chen[1,2,3], and Min Chen[1,2*]

[1]Department of Chemistry, [2]Molecular and Cellular Biology Program, and [3]Department of Biochemistry and Molecular Biology, University of Massachusetts Amherst, Amherst, Massachusetts 01003, USA

*E-mail: mchen1@chem.umass.edu. Phone: (413) 545-0683.

Contents

Supplementary information figures……..……3

Supplementary Figure 1. Kinetic analysis of MBP trapped in ClyA. ……..……3
Supplementary Figure 2. MBP trapped in ClyA. ……..…..4
Supplementary Figure 3. Frequencies of the three MBP-bound states in varied concentrations of maltose or maltotriose. ……...…….....……5
Supplementary Figure 4. Detection of MBP with non-substrates and substrates by nanopore. ..……6
Supplementary Figure 5. Simulation. ..…….……7
Supplementary Figure 6. Two schemes for interpreting the multiple current levels of MBP trapped within ClyA. ..……..…….……8
Supplementary Figure 7. ITC assay for MBP/maltose binding affinities. ..……9
Supplementary Figure 8. The anomeric binding affinities of MBP. ……10
Supplementary Figure 9. Calculation of the dwell time of the three ligand-bound states. …..11
Supplementary Figure 10. Dissociation time of ligands from MBP exposed to various ligand concentrations in three binding modes. ……..……12
Supplementary Figure 11. Structure of the ligand binding pocket of MBP. ……...13
Supplementary information table 1……14

Supplementary information figures

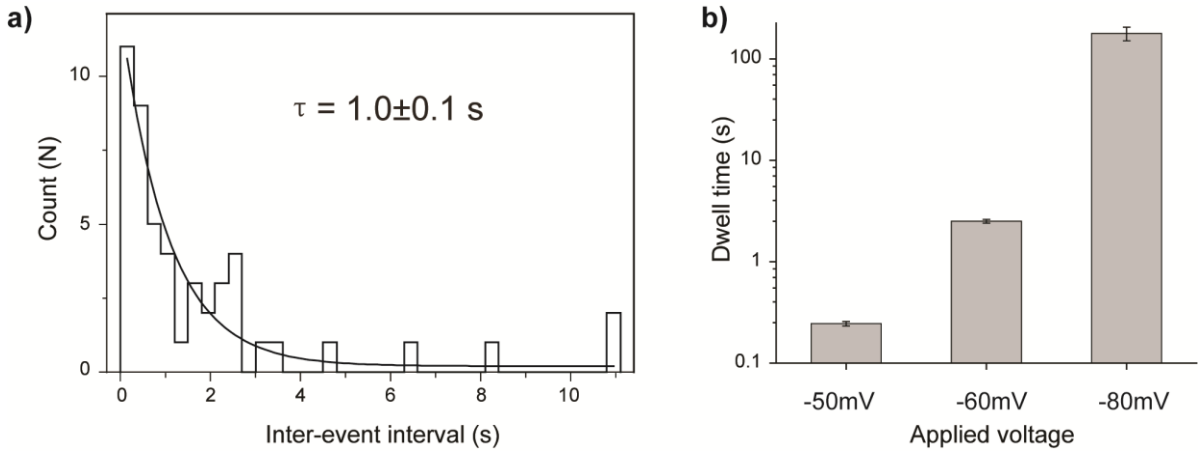

Supplementary Figure 1. Kinetic analysis of MBP trapped in ClyA. (a) The histogram shows the inter-event interval of 56 nM MBP interacting with the nanopore under -80 mV (n= 49) and fitted with standard exponential function. (b) The dwell time of 56 nM MBP interacting with the nanopore under -50 mV (n= 96), -60 mV (n= 45) and -80 mV (n= 49)

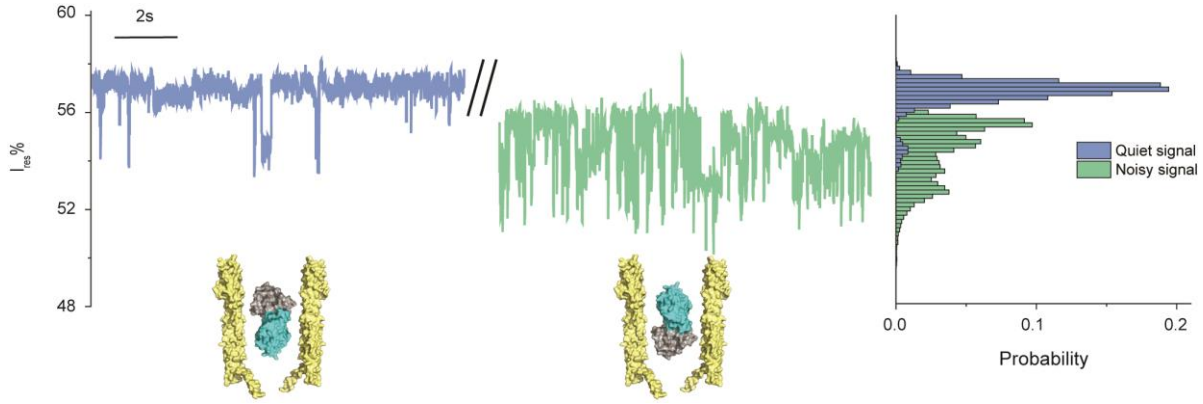

Supplementary Figure 2. MBP trapped in ClyA. Two electrical patterns observed for MBP trapped in ClyA nanopore. There was ~ 60 % chance to see the quiet signal (blue), which responded to the ligand binding and were selected in the following analysis. The noisy signal (green) has a smaller I_{res} % and represents the pattern that didn't respond to the ligand binding. The histogram on the right shows the corresponding histogram of the two trapping patterns.

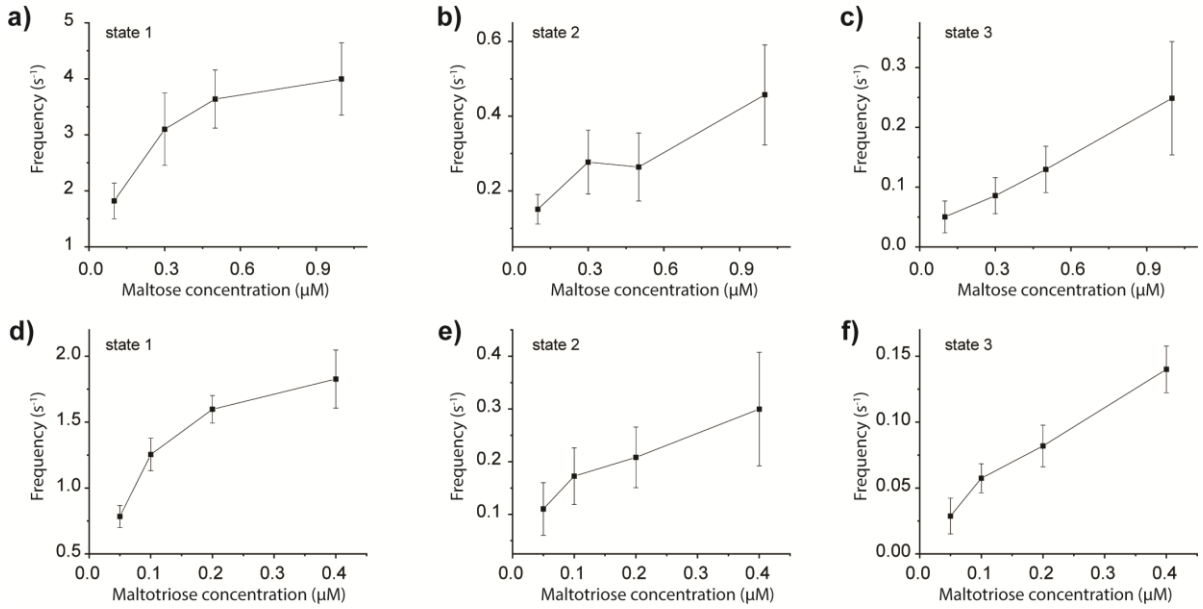

Supplementary Figure 3. Frequencies of the three MBP-bound states in varied concentrations of maltose or maltotriose. The state frequencies collected from multiple MBP/maltose and MBP/maltotriose trapping experiments were shown in (a-c) and (d-f) separately as the average SD. All the measurements were performed in 150 mM NaCl, 15 mM Tris-HCl, pH 7.5 with -80 mV applied in *trans*. Detailed information was listed in Supplementary Table 1.

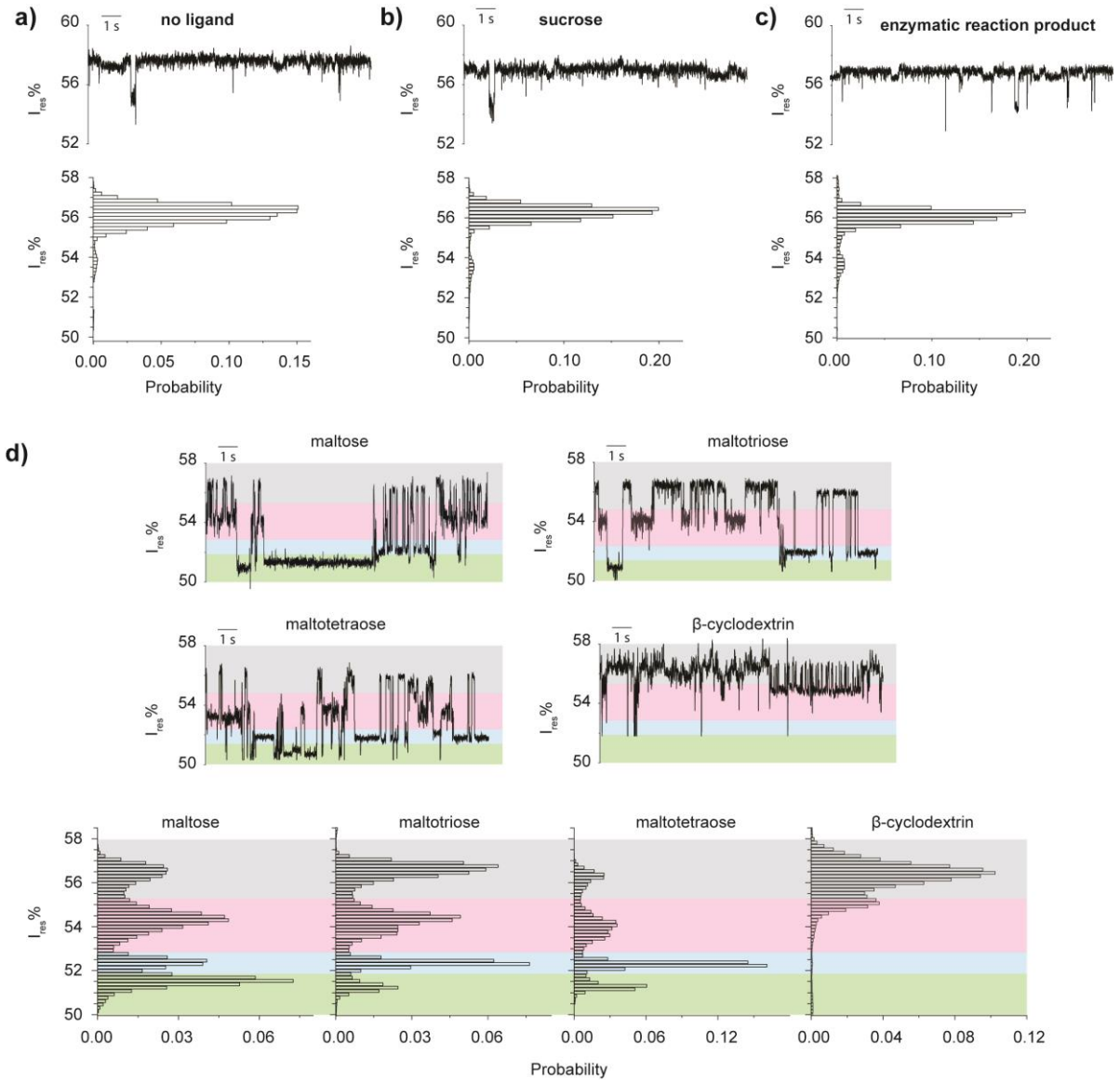

Supplementary Figure 4. Detection of MBP with non-substrates and substrates by nanopore. (a) Representative trace and blockades histogram of individual MBP confined inside ClyA. (b) Typical trace and blockades histogram of MBP with 1 μM sucrose added in the *cis* chamber measured by ClyA. (c) Representative trace and blockades histogram of MBP after addition of enzymatic reaction product with ClyA. 2 mM maltose and 2 mM sodium phosphate were incubated with 1 unit of maltose phosphorylase overnight at room temperature to obtain the concentrated reaction product. The reaction mixture (5 μl) was then diluted by 200-fold by cis buffer (150 mM NaCl, 15 mM Tris-HCl, pH 7.5). (d) Typical trace and blockades histograms of MBP with 1 μM maltose or 0.2 μM maltotriose or 0.5 μM maltotetraose or 2.5 μM β-cyclodextrin added in the *cis* chamber detected by ClyA. The current was colored into 4 states according to the state assignment in MBP/maltose interactions. All measurements were performed n 150 mM NaCl, 15 mM Tris-HCl, pH 7.5 by applying a Bessel low-pass filter with a 2 kHz cutoff and sampled at 5 kHz.

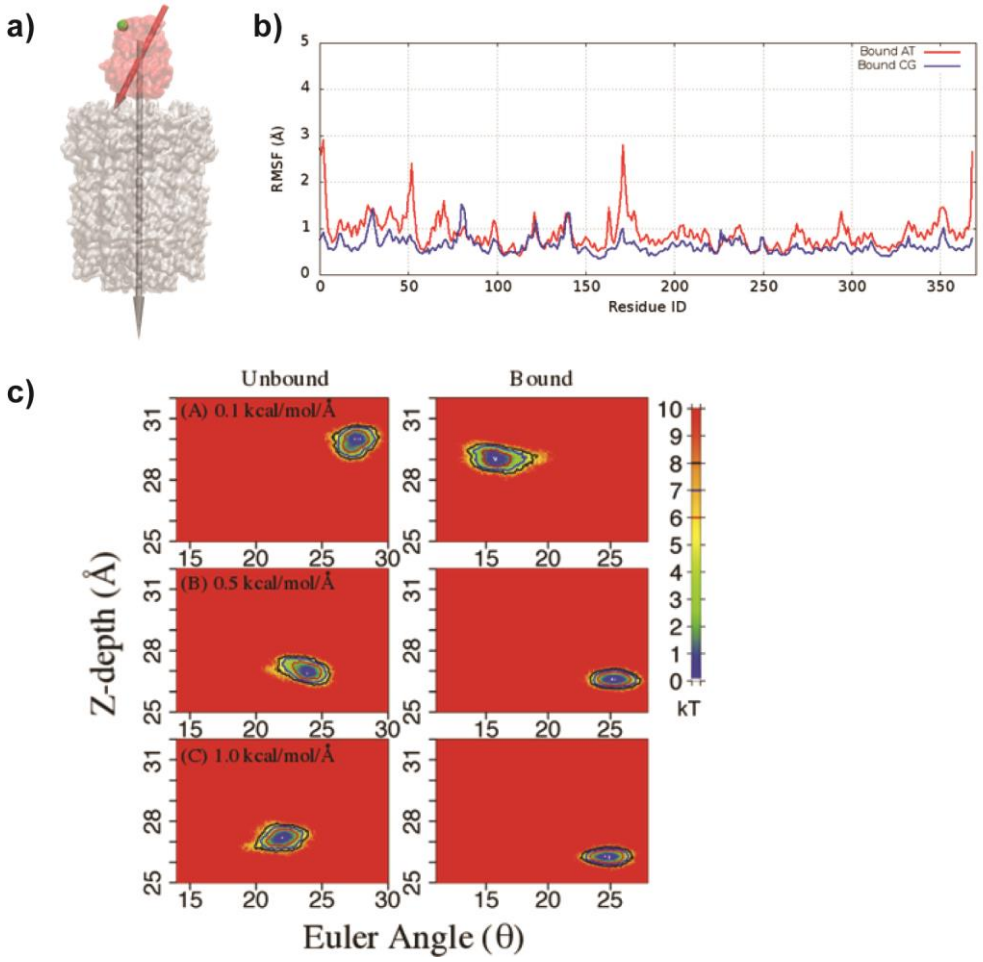

Supplementary Figure 5. Simulation. (a) Orientation of electric dipoles of ClyA and maltose-bound MBP. Both ClyA and MBP are aligned to their principle axis. The color code for ClyA and MBP are grey and red, respectively. The green sphere represents the N-terminus. In this configuration, the N-terminus is facing up. (b) The root-mean-square fluctuation (RMSF) profiles of MBP calculated from 50 ns atomistic (red) and coarse-grained (blue) simulations. (c) Free energy surface using z-depth and Euler angle θ for three force constants 0.1, 0.5, and 1.0 kcal/mol/Å. The left and right columns are from unbound and bound MBP simulations. The contour levels in red, blue and black are for 6, 7 and 8 kT respectively. The last 250 ns data of each simulation is used for data analysis.

a) Single ligand bound MBP confomer (PL) interacting with ClyA forming three complexes (PL•ClyA$_1$, PL•ClyA$_2$, PL•ClyA$_3$)

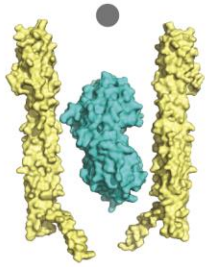

$$P + L \rightleftharpoons PL$$

$$PL + ClyA \rightleftharpoons PL{\bullet}ClyA_1 \qquad K_{d1} = \frac{[PL] \times [ClyA]}{[PL{\bullet}ClyA_1]}$$

$$PL + ClyA \rightleftharpoons PL{\bullet}ClyA_2 \qquad K_{d2} = \frac{[PL] \times [ClyA]}{[PL{\bullet}ClyA_2]}$$

$$PL + ClyA \rightleftharpoons PL{\bullet}ClyA_3 \qquad K_{d3} = \frac{[PL] \times [ClyA]}{[PL{\bullet}ClyA_3]}$$

$$[PL{\bullet}ClyA_1]:[PL{\bullet}ClyA_2]:[PL{\bullet}ClyA_3] = \frac{1}{K_{d1}} : \frac{1}{K_{d2}} : \frac{1}{K_{d3}}$$

b) Three ligand bound MBP conformers (PL_1, PL_2, PL_3)

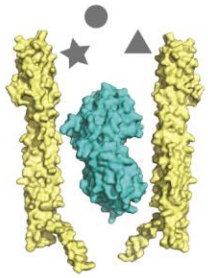

$$P + L_1 \rightleftharpoons PL_1 \qquad K_{d1} = \frac{[P] \times [L_1]}{[PL_1]} = \frac{[P] \times ([L_1]^T - [PL_1])}{[PL_1]}$$

$$P + L_2 \rightleftharpoons PL_2 \qquad K_{d2} = \frac{[P] \times [L_2]}{[PL_2]} = \frac{[P] \times ([L_2]^T - [PL_2])}{[PL_2]}$$

$$P + L_3 \rightleftharpoons PL_3 \qquad K_{d3} = \frac{[P] \times [L_3]}{[PL_3]} = \frac{[P] \times ([L_3]^T - [PL_3])}{[PL_3]}$$

$$[PL_1]:[PL_2]:[PL_3] = \frac{[L_1]^T}{K_{d1} + [P]} : \frac{[L_2]^T}{K_{d2} + [P]} : \frac{[L_3]^T}{K_{d3} + [P]}$$

Supplementary Figure 6. Two schemes for interpreting the multiple current levels of MBP trapped within ClyA. (a) A single ligand loaded MBP conformer (PL) interacts with ClyA in three ways to form PL•ClyA$_1$, PL•ClyA$_2$ and PL•ClyA$_3$. (b) Three different ligands interact with MBP to form three distinct conformers: PL_1, PL_2 and PL_3. $[L_i]^T$ represents the total concentration of each ligand in solution.

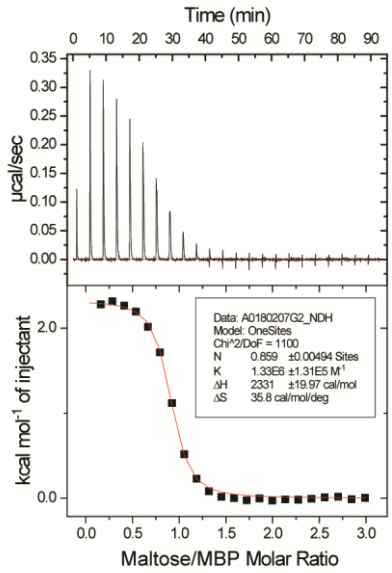

Supplementary Figure 7. Isothermal titration calorimetry assay for MBP/maltose binding affinities. Calorimetric titration curves obtained for MBP bound to maltose at 25 ° C. MBP concentration was 69 µM. The titration of 1035 µM maltose included one initial injection of 0.5 µL, followed by 22 injections of 1.7 µL each. The stirring speed is 800 rpm and spacing time between injections is set to 240 s to allow the signal caused by titration to return to the baseline. Data were analyzed with the software provided by the supplier.

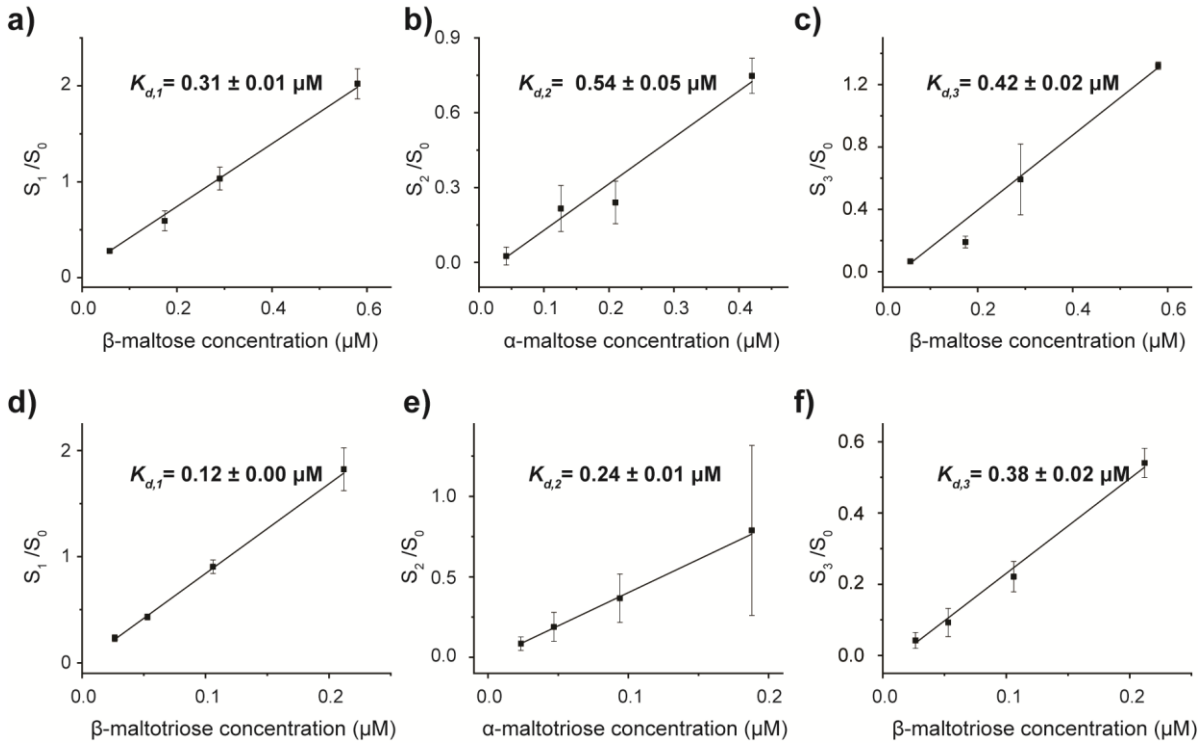

Supplementary Figure 8. The anomeric binding affinities of MBP. The binding affinities (Kd) for MBP bound to maltose (a-c) and maltotriose (d-f) in three binding modes were derived as described in supplementary text (determination of dissociation constant). Briefly, the binding affinity was acquired by inverting the slope of linear fitted graph of S_i/S_0 against the concentration of the corresponding anomer. S_i indicates the area of that state and S_0 indicates the area of the unbound state. The concentration of α-anomer and β-anomer concentration can be obtained according to their ratio in the equilibrated maltose or maltotriose solution.

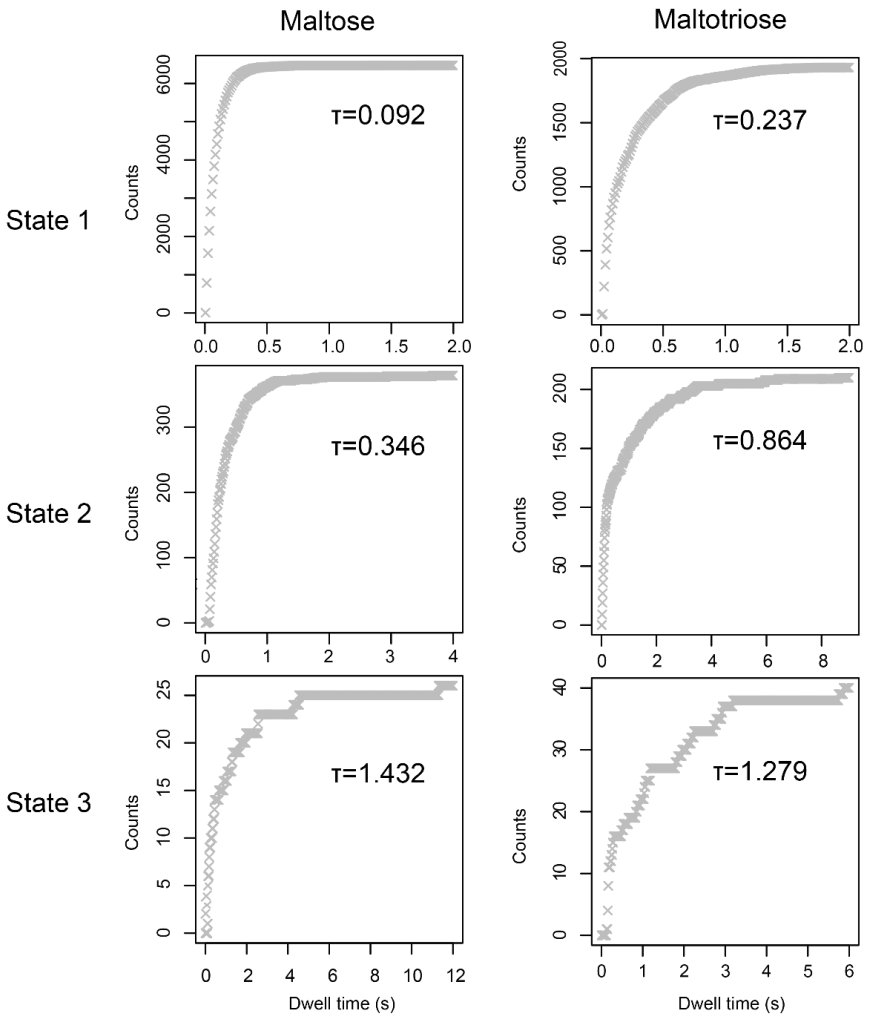

Supplementary figure 9: Representative cumulated histograms of the dwell time of the three states. The histograms were used to calculate the mean first passage time. The same analysis protocol was applied to different experimental trace.

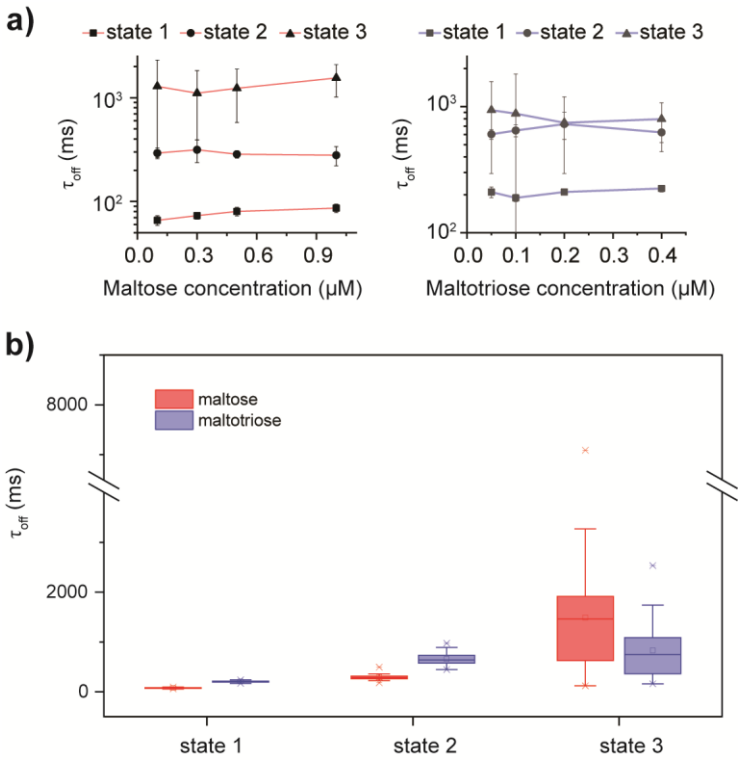

Supplementary Figure 10. Dissociation time of ligands from MBP exposed to various ligand concentrations in three binding modes. (a) The relationship between dissociation time (τoff) and ligand concentration in state 1 (■), state 2 (●) and state 3(▲). The MBP binding to maltose was shown in red and the binding to maltotriose was represented in blue. (b) The parallel comparison of between MBP bound with maltose and maltotriose. The dissociation time were the combined results from that binding mode regardless of the ligand concentration. The MBP binding to maltose was shown in red and the binding to maltotriose was represented in blue.

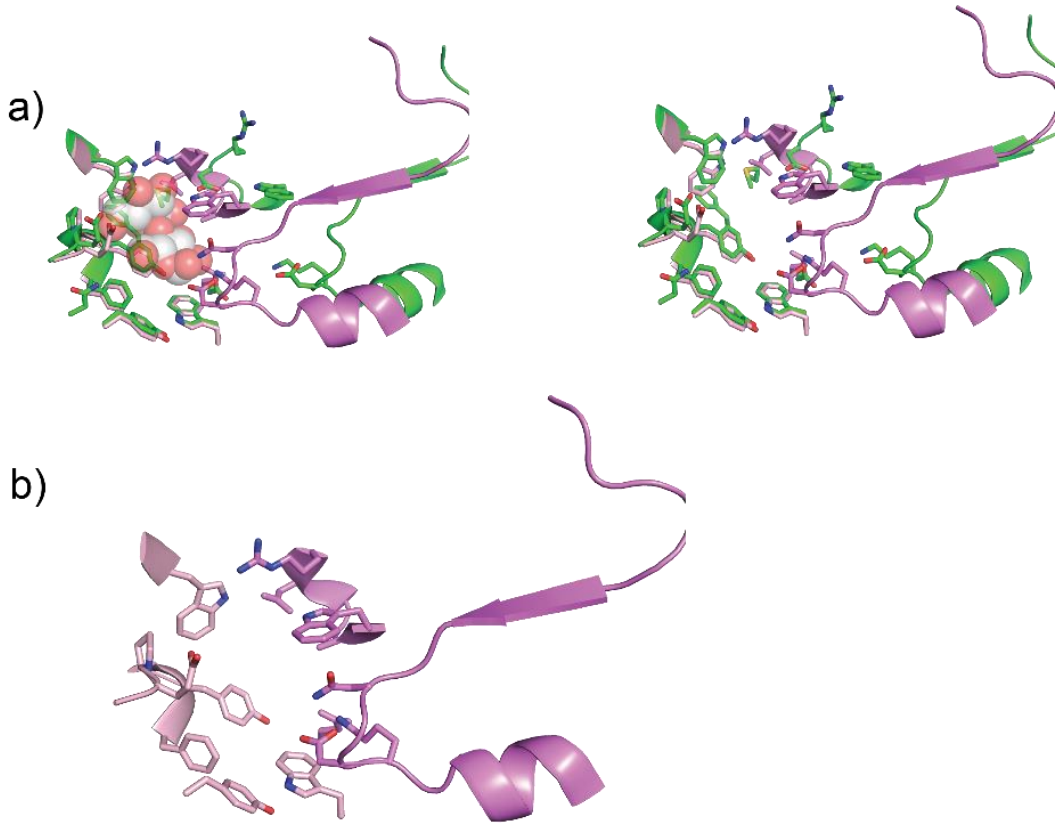

Supplementary Figure 11. Structures of the ligand-binding pocket of MBP at different states. **a**) Structural alignment of the ligand binding sites at the unbound (green, pdb: 1jw4) and maltose bound state (pink, pdb: 1anf). The maltose molecule is shown in a sphere model at the left panel and taken out at the right panel. **b**) Structure of the ligand binding site of the maltose bound state (1anf). Residues at the CTD are labeled in light pink and the ones at the NTD in violet.

Supplementary table S1: Events collected from different MBP individuals trapped in ClyA exposed to various maltose or maltotriose concentration.

Ligand	Concentration	MBP Dwell Time (s)	Events of state 1	Events of state 2	Events of state 3
maltose	0.1 µM	816	1691	63	15
		928	1899	115	25
		392	630	74	14
		1063	2364	215	53
		1164	1655	180	40
		399	592	54	37
		823	1334	122	67
		820	1698	143	51
	0.3 µM	653	2390	143	53
		616	2328	160	48
		183	691	26	4
		910	2417	369	106
		569	1515	194	56
		987	2772	275	80
		478	1628	168	56
		488	998	107	45
	0.5 µM	613	1762	71	45
		179	600	55	25
		660	2955	241	61
		395	1630	110	43
		279	1109	46	35
		1000	3443	316	153
		997	3548	208	197
		993	3263	352	146
	1.0 µM	1018	5525	647	430
		817	3186	290	127
		1588	6831	586	244
		851	3204	335	155
		454	1633	283	93
		551	1976	176	183
		1207	4093	712	351
		1082	4329	403	269
maltotriose	0.05 µM	432	381	53	19
		300	204	40	8
		608	469	90	20
		2101	1686	78	24
	0.1 µM	1314	1436	308	94

		294	401	59	18
		633	731	122	39
		312	407	32	15
		918	1243	121	41
	0.2 µM	445	682	114	37
		455	739	90	29
		611	868	167	59
		339	582	38	26
		532	869	99	36
		1052	1742	235	109
	0.4 µM	339	513	156	56
		780	1491	189	108
		319	592	84	42
		1018	2062	237	127